Quantum Electronics **39** (4) 347 – 352 (2009)

LIGHT MODULATION

PACS numbers: 42.30.Va; 42.79.Jq
DOI: 10.1070/QE2009v039n04ABEH013904

Wide-aperture diffraction of unpolarised radiation in a system of two acousto-optic filters

L.N. Magdich, K.B. Yushkov, V.B. Voloshinov

***Abstract*. Light diffraction is studied in two tandem acousto-optic cells filtering unpolarised radiation with a wide angular spectrum. It is shown that the side lobes of the ultrasonic radiation pattern of a piezoelectric transducer produce side diffraction intensity maxima at the output of the system consisting of two filters. Diffraction in paratellurite filters is studied experimentally at 1.06 μm.**

Keywords: *paratellurite, successive acousto-optic diffraction, wide-aperture acousto-optic filter, modulation of unpolarised radiation.*

1. Introduction

Light diffraction on phase gratings induced by ultrasonic waves finds wide applications in systems processing optical signals and controlling the parameters electromagnetic radiation. At present, many acousto-optic (AO) devices are based on crystalline materials with the anisotropy of elastic and electromagnetic properties. It is known that in anisotropic light diffraction used in AO filters, it is necessary to couple light with a certain direction of linear polarisation to the AO cell input [1 – 3]. In the general case, when arbitrary-polarised light is incident on the AO crystal, a significant part of the optical energy can be concentrated in the eigenmode, for which the phase-matching condition is not fulfilled. To process unpolarised radiation, different AO systems were proposed, which make use of the optical properties of crystals [4, 5], peculiarities of the anisotropic Bragg diffraction of light [6 – 9] or excitation of several sound waves of different directions in the crystal [10].

It is known that the use of several AO filters placed in tandem along the propagation of light allows one to increase the diffraction efficiency, to decrease the system transmission band due to the increase in the interaction length of the light and sound waves as well as to considerably suppress the side maxima of the device transmission function [11, 12]. Multiple propagation of light through one AO cell can improve the parameters of the filtering system [5, 13]. In this paper, we studied the diffraction of unpolarised light beams with a wide angular spectrum in a system consisting of two identical AO filters placed in tandem. The AO system configuration under study was first proposed in [14]. A wide-aperture Bragg diffraction regime in paratellurite was used to process beams with a wide angle spreading [15]. The advantage of this system is the possibility to use the zero and first diffraction orders, which allows one to fabricate bandpass and band-stop filters and modulators of uncollimated light beams.

L.N. Magdich Federal State Unitary Enterprise, M.F. Stel'makh Polyus Research and Development Institute, ul. Vvedenskogo 3, 117342 Moscow, Russia;
K.B. Yushkov, V.B. Voloshinov Department of Physics, M.V. Lomonosov Moscow State University, Vorob'evy gory, 119992 Moscow, Russia; e-mail: volosh@phys.msu.ru

Received 8 May 2008; revision received 19 August 2008
Kvantovaya Elektronika **39** (4) 347 – 352 (2009)
Translated by I.A. Ulitkin

2. Light diffraction from several Bragg gratings

It is known that the law of conservation of momentum during the AO interaction of light can be illustrated with the help of the wave-vector diagram [1]. Figure 1 shows the vector diagram in the case of a uniaxial crystal in which unpolarised light of wavelength λ propagates in air. The diagrams describe refraction and AO scattering of light in the principal plane of crystalline samples with parallel optical faces and the piezoelectric transducer plane inclined at an angle α to the optical axis. The subscripts 'i' and 'd' correspond to the incident and diffracted light and subscripts 1 and 2 – to the wave vectors in the first and second crystals, respectively, the subscripts 'o' and 'e' – the ordinary and extraordinary polarisations of optical eigenmodes in crystals. If arbitrary polarised radiation with the wave vector $\boldsymbol{k}_{\mathrm{i}}'$ is incident on the crystal with the major refractive indices n_{o} and n_{e} (hereafter, the primed quantities are the angles and vectors in air and the unprimed quantities are angles and vectors in the medium), two waves with different polarisations will propagate in the crystal. In this case, the group velocity of an extraordinary polarised wave is determined by its ray vector $\boldsymbol{s}_{\mathrm{i1}}$ and is directed at an angle to the wave vector $\boldsymbol{k}_{\mathrm{i1}}^{\mathrm{e}}$ [3].

If an ultrasonic wave with the front making the angle α with the crystal optical axis is excited in the crystal, by selecting the ultrasound frequency f the phase-matching condition can be fulfilled separately for radiation of each optical eigenmode in the crystal [3]. Figure 1a presents the vector diagram of the AO diffraction for which the Bragg matching conditions is fulfilled for the e-polarised light. Usually, a polarised wave does not experience diffraction in this case and propagates through the cell without any changes in its intensity because the phase-matching condition for it is not fulfilled at the same frequency and direction of the ultrasonic wave. The vector equation describing diffraction in the first AO cell has the form

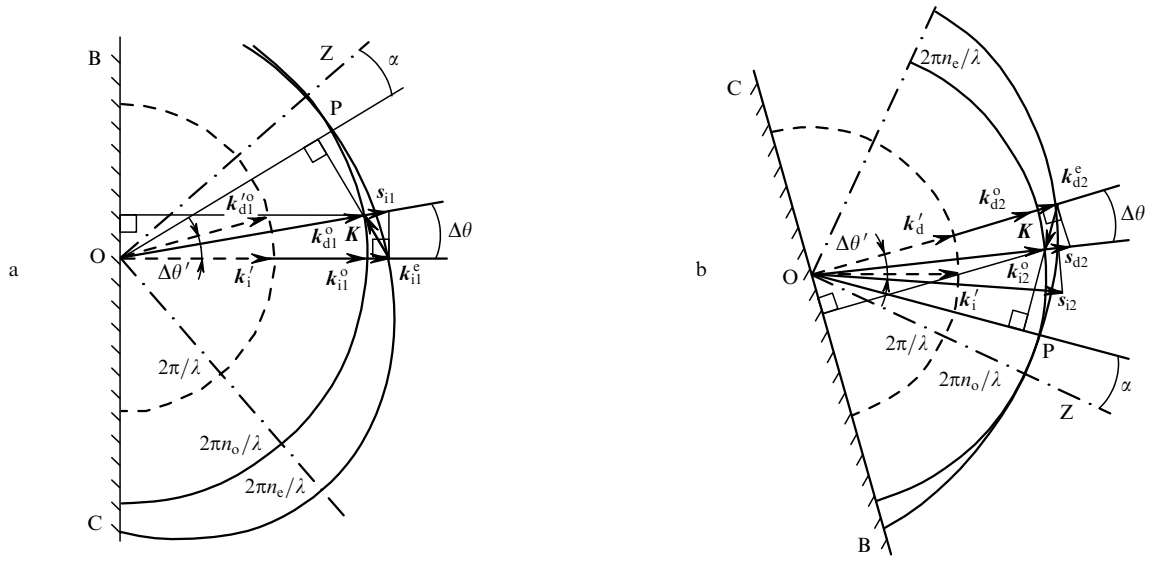

Figure 1. Vector diagrams of wide-angle diffraction of unpolarised light in the first (a) and second (b) cells: OZ are optical axes of crystals; OP are piezoelectric transducer planes; BC are planes of the input and output faces of crystals.

$$\boldsymbol{k}^{e}_{i1} + \boldsymbol{K} = \boldsymbol{k}^{o}_{d1}, \tag{1}$$

where $\boldsymbol{K}$ is the wave vector of the ultrasonic wave.

In the case, when the wave vector direction $\boldsymbol{k}^{o}_{d1}$ of diffracted light coincides with the beam vector direction $\boldsymbol{s}_{i1}$ of incident light, the AO interaction geometry is wide-angle one [15, 16]. In a filter with a wide-angle configuration, the deviation angle $\Delta\theta$ of diffracted light inside the crystal is equal to the 'walk-off' angle of the e-polarised wave and in air the deviation angle at the crystal output is $\Delta\theta' = \arcsin(n_o \sin\Delta\theta) \approx n_o\Delta\theta$.

The scheme of the ray path in the AO system under study is shown in Fig. 2. Arbitrary polarised ray 1 with the wave vector $\boldsymbol{k}'_{i}$ is split into rays 2 and 3 with o- and e-polarisations, respectively. Ray 3 experiences diffraction in the first AO cell according to equation (1). As a result, diffracted ray 4 is produced. In addition, at the output of the first AO cell, side diffracted ray 5 can be observed, which appears due to the Bragg diffraction at the side components of the ultrasonic wave if the phase-matching condition is violated [1]. The parameters of side diffraction maxima are discussed in section 5.

One can see from Fig. 1 that the planes of the input and output faces of the first crystal are oriented orthogonally to the direction of incident light. In this case, at the output of the first AO cell, the propagated beams of both polarisations will propagate parallel to each other at a distance $l_c \tan\Delta\theta$ caused by the material birefringence, where l_c is the crystal length.

To fulfil the phase-matching condition for the o-polarised wave (ray 2), the second AO cell should be rotated by the angle $\Delta\theta'$ with respect to the first cell. If in this case the second AO cell is rotated by 180°, the propagation direction of diffracted e-polarised ray 7 with the wave vector $\boldsymbol{k}^{e}_{d2}$ will almost coincide at the output with the direction of the wave vector $\boldsymbol{k}^{o}_{d2}$ of ordinary polarised ray 4 emerging due to diffraction in the first AO cell. In this case, scattering described by the equation

$$\boldsymbol{k}^{o}_{i2} - \boldsymbol{K} = \boldsymbol{k}^{e}_{d2} \tag{2}$$

occurs to the −1 order. Figure 1b shows the diffraction pattern in the second AO filter.

In the second cell, radiation in the zero and first diffraction orders (rays 3 and 4 in Fig. 2) will refract without diffraction and have wave vectors $\boldsymbol{k}^{e}_{i2}$ and $\boldsymbol{k}^{o}_{d2}$, respectively (Fig. 1b). Thus, as was noted earlier in [14], at the system output rays 4 and 7 will propagate parallel with some spatial displacement. If AO cells are separated by Δl from each other, the distance Δx between the rays will be $\sim (2l_c + n_o\Delta l)\Delta\theta$ (Fig. 2).

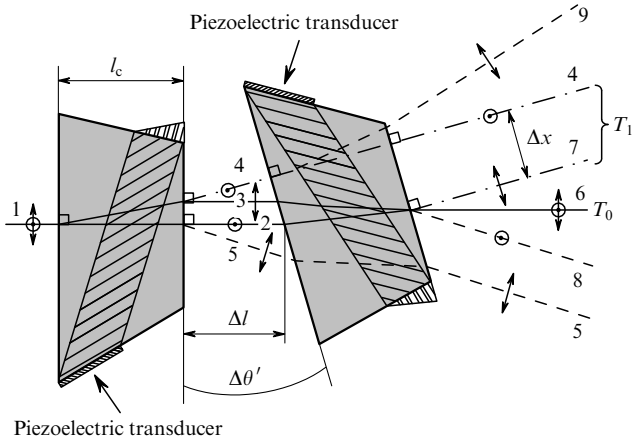

Figure 2. Scheme of the ray path in the system of AO filters. Dot-and-dash straight lines are diffracted rays; dashed lines are rays of side diffraction maxima.

A diffracted e-polarised wave propagates in the second AO cell with the ray vector $\boldsymbol{s}_{d2}$, whose direction coincides with the wave vector direction $\boldsymbol{k}^{o}_{i2}$ of the incident wave in the crystal. In addition, an e-polarised wave (ray 3) with the ray vector $\boldsymbol{s}_{i2}$ and wave vector $\boldsymbol{k}^{e}_{i2}$ will propagate in the zero diffraction order in the second crystal. The walk-off direction of this wave in the second crystal is such that at the system output rays 2 and 3 corresponding to the zero

diffraction order prove to be spatially combined and produce ray 6, whose polarisation coincides with that of incident ray 1. Thus, the use of two identical crystals turned by the angle close to 180° allows one to compensate for the splitting of an arbitrary polarised light beam into two linearly polarised beams, splitting being caused by the birefringence of the AO medium material. As in the first AO filter, side rays 8 and 9, which appear in the light diffraction due to the side lobes of the transmission function, can be produced in the second cell.

Because only one of radiation eigenmodes in the crystal diffracts in each of the AO cells, the parameters of diffracted light are determined only by the properties of only one of the AO cells. In this case, the other cell for these waves is a plane-parallel birefringent plate, which spatially displaces the light beam without changing its propagation direction. Nevertheless, diffraction in both AO cells occurs at one and the same ultrasound frequency, which makes it possible to feed the system with only one high-frequency signal generator by connecting it simultaneously to both cells.

3. Acousto-optic diffraction upon violation of the phase-matching condition

It is known that because the interaction region of the light and sound waves is limited, the Bragg regime of AO diffraction is observed in the finite frequency band of acoustic waves [1]. At high ultrasound frequencies corresponding to the Bragg regime of light diffraction, projector propagation of ultrasound waves is observed in crystals; therefore, we can consider the light scattering in a plane-parallel acoustic column of length $l = l_{\mathrm{PT}} \cos\psi$ (l_{PT} is the piezoelectric transducer length and ψ is the angle between the directions of the group and phase velocities of ultrasound). In this case, when the Bragg condition is violated, we can use the phase mismatch vector $\boldsymbol{\eta}$, which is orthogonal to the ray vector of the ultrasound wave. The modulus of the vector mismatch η is determined by the AO interaction efficiency [1]:

$$T_1 = \frac{q^2}{q^2+\eta^2} \sin^2\left[\frac{l}{2}\left(q^2+\eta^2\right)^{1/2}\right], \tag{3}$$

where the parameter q is proportional to the sound wave amplitude. It is obvious that the transmission function for radiation in the zero diffraction order in the Bragg regime is determined by the quantity $T_0 = 1 - T_1$ in the absence of multiple scattering. The maximum scattering efficiency $T_1 = 1$ is observed when the phase-matching condition is exactly fulfilled ($\eta = 0$) and the ultrasound power, to which $q = \pi/l$ corresponds, is optimal. If we introduce the dimensionless mismatch $H = \eta l/\pi$, it is easy to obtain from (3) the transmission function of the AO filter operating in the regime of the maximum diffraction efficiency:

$$T(H) = \frac{\pi^2}{4} \operatorname{sinc}^2\left[\frac{1}{2}\left(1+H^2\right)^{1/2}\right]. \tag{4}$$

This function is fast decaying and oscillating, more than 75 % of the energy transmitted by radiation being concentrated in the region of the central maximum, which is limited by the condition $|H| \leqslant \sqrt{3}$. The double decrease in the intensity compared to its maximum value is observed at the mismatch $H \approx \pm 0.8$ and the quantity of the first side maximum at $H = \pm\sqrt{8}$ achieves 0.11 [1].

Transmission function (4) allows one to calculate the filter transmission bandwidth $\Delta\lambda$ upon illumination by broadband electromagnetic radiation at a fixed ultrasound frequency f, and the ultrasound frequency bandwidth Δf in which diffraction of monochromatic light is observed. In this case, relative quantities $\Delta\lambda/\lambda$ and $\Delta f/f$ are equal to each other and can be determined by the expression

$$\frac{\Delta\lambda}{\lambda} = \frac{\Delta f}{f} = \frac{0.8V}{l_{\mathrm{PT}} f}\left[\tan\psi + \cot(\theta_{\mathrm{B}} - \Delta\theta)\right], \tag{5}$$

where θ_{B} is the Bragg angle of light incidence and V is the phase velocity of ultrasound.

4. Experimental

As main dispersion elements we used two identical trapezium-shape AO cells based on single-crystal paratellurite (TeO_2). To ensure the cell identity, they were made from the same crystal, which provided the exact equality of cut-off angles in both crystals and inclination angles of their optical faces. An elastic wave of a slow shear mode was excited in crystals by x-cut piezoelectric lithium niobate plates of length $l_{\mathrm{PT}} = 1.1$ cm. The wave vector direction $\boldsymbol{K}$ of the ultrasound wave made an angle $\alpha = 10°$ to the [110] crystallographic axis in the $(\bar{1}10)$ plane, which ensured a high quality of the AO material in the chosen direction at the ultrasound velocity $V \approx 7.1 \times 10^4$ m s^{-1} [2]. The input and output optical faces of the crystal were cut parallel to each other and made an angel of 76.5 % to the crystal optical axis. Thus, at the normal incidence of light on the crystal input face, the wide-angle Bragg diffraction condition was fulfilled for e-polarised radiation; the wide-angle diffraction of o-polarised radiation was provided at the same ultrasound frequency for the ray with the incidence angle $\Delta\theta' \approx 6°$. The crystal length in the direction of light propagation was $l_{\mathrm{c}} = 3.0$ cm, and the linear size of the aperture was chosen equal to 0.7×0.8 cm.

Both crystals were mounted in the same housing due to which the mutual position of the AO cells was fixed so that in the case of fulfilment of the wide-angle Bragg diffraction condition in the first cell for radiation with one polarisation, wide-angle diffraction with the opposite polarisation should be observed in the second cell. It is obvious that if incident radiation falls on the input face of the first crystal at an angle $\Delta\theta'$, the wide-angle diffraction condition in the first cell will be fulfilled for o-polarised radiation at the same ultrasound frequency f^* as that in the case of normal incidence of light on the AO cell. In this case, the e-polarised field component is diffracted in the second filter. When the AO cells are separated by $\Delta l = 0.5$ cm, the distance Δx between rays 4 and 7 was ~ 3.4 mm. When wide light beams are used, whose size is only limited by the linear aperture of the AO cells, there occurs a significant overlap of the rays in the first diffraction order.

The system was powered with high-frequency signals from a generator with a power divider at its output, which provided the same amplitude of the acoustic wave in both crystals. Diffraction of 1.064-μm radiation from an Nd : YAG laser was observed at the ultrasound frequency $f^* = 65.75$ MHz. The highest diffraction efficiency T_1 achieved 95 % at the sound wave power $P = 1.0$ W in

each AO cell. Thus, at the maximum diffraction efficiency the total power consumed by the system was 2 W.

The filter transmission band $\Delta\lambda$ at the -3-dB level was 5.0 nm at the radiation wavelength $\lambda = 1.06$ μm, which yields the spectral resolution $r = \Delta\lambda/\lambda^2 \approx 46$ cm^{-1}. The ultrasound frequency band $\Delta f = 0.3$ MHz during monochromatic illumination corresponds to the interaction length $l \approx 0.8$ cm of the light and sound waves, which, at the acoustic 'walk-off' angle of $\psi = 54$ allows one to determine by using expression (5) the effective length l_{PT} of the piezoelectric transducer equal to ~ 1.3 cm. This length hardly differs from the real size of the transducer (1.1 cm). The instrument function of this system of AO filters is shown in Fig. 3. One can see from Fig. 3a that the scattering of unpolarised radiation in the zero order is observed not only at the fundamental frequency of ultrasound $f^* = 65.75$ MHz but also at the frequency $f \approx 67.0$ MHz. The second minimum of the transmission function corresponds to diffraction of polarised rays for which the matching condition at the same angle of light incidence is fulfilled for a higher ultrasound frequency than in the case of wide-angle diffraction under study. This scattering occurs in the diffraction order which is opposite from the main (wide-angle) one and, therefore, does not affect the instrument function of the first scattering order shown in Fig. 3b.

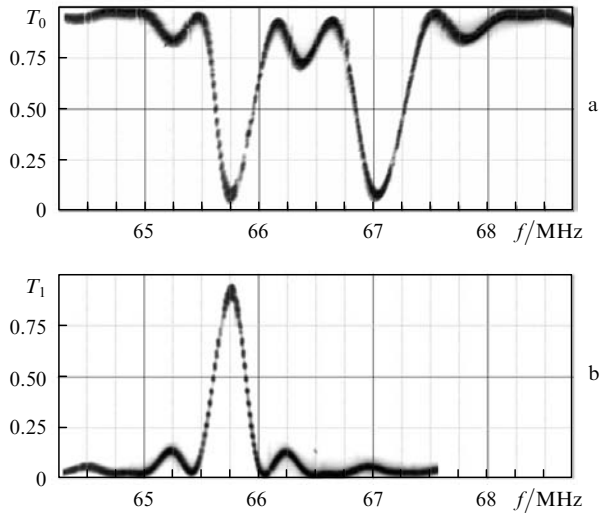

Figure 3. Measured transmission function of the filtration system in the zero (a) and first (b) diffraction orders upon illumination by arbitrary polarised light.

5. Formation of side diffraction maxima

In filtering AO systems processing linearly polarised radiation, the initial light wave propagates through polarisers before entering the AO crystal [11, 13, 15, 16]. Unlike this case, in our filter scheme of unpolarised radiation, light beams with both polarisations propagate through the AO cells. In this case, the phase-matching condition in the first cell is not fulfilled for the light field component with the o-polarisation. However, in the case of ordinary polarised light we can observe weaker diffraction provided by the side components of the sound beam, to which side lobes of the transmission function of the AO filter correspond. For example, in the vector diagram shown in Fig. 1a, the wave vector equal to $\boldsymbol{k}_{i1}^{o} - \boldsymbol{K}$ does not meet the matching condition in the crystal; however, diffraction of the o-polarised ray is possible due to the side component of the radiation pattern in the piezoelectric transducer.

Figure 4 presents the dependences of the phase-matching frequency f on the Bragg angle θ_B in the vicinity of the exact angle of the wide-angle diffraction, which are calculated with the help of vector relations (1) and (2). At the ultrasound frequency $f^* = 65.75$ MHz, the Bragg angle for the o-polarised wave is $\theta_B^o = 10.7^\circ$ and for the e-polarised wave – $\theta_B^e = 13.2^\circ$. The frequency corresponding to the wide-angle Bragg diffraction decreases with decreasing the cut-off angle α. For example, if we consider light diffraction on the sound field component propagating at the angle $\alpha \approx 9.92^\circ$, the phase-matching condition for the o-polarised light will be fulfilled at the same ultrasound frequency and the same Bragg angle as that in the case of wide-angle diffraction of the e-polarised wave. However, this diffraction is not wide-aperture and will proceed in the -1 order. Similarly, for diffraction of e-polarised light in the $+1$ order, the phase-matching condition will be fulfilled at the same angle as that in the case of wide-angle diffraction of the o-polarised wave on the acoustic field component with the propagation angle $\alpha \approx 9.89^\circ$. Frequency-angular parameters during diffraction of light by these side components of the radiation pattern are shown in Fig. 4 for $\delta\alpha^o \approx -0.08^\circ$ ($\alpha = 9.92^\circ$) and $\delta\alpha^e \approx -0.11^\circ$ ($\alpha = 9.89^\circ$).

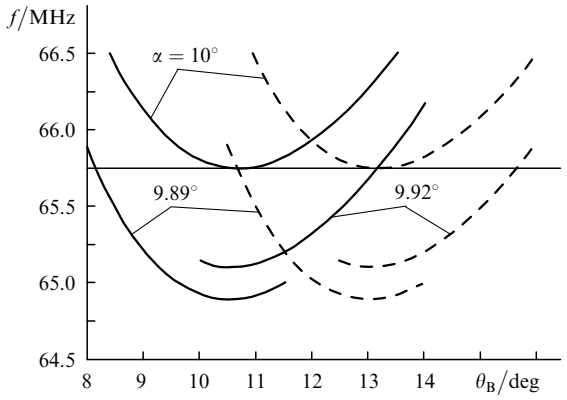

Figure 4. Dependences of the acoustic frequency f on the Bragg angle θ_B at different directions of the wave vector of the ultrasound wave for the ordinary (solid curves) and extraordinary (dashed curves) polarisations of incident radiation.

Vector diagrams of radiation diffraction into side maxima are presented in Fig. 5. The subscript 'a' corresponds to rays produced during side scattering of light. Light diffraction on side components of the angular spectrum of the acoustic wave is described by three vector equations:

$$\begin{aligned} \boldsymbol{k}_{a1}^{e} &= \boldsymbol{k}_{i1}^{o} - \boldsymbol{K} - \boldsymbol{\eta}^{o}, \\ \boldsymbol{k}_{a2}^{e} &= \boldsymbol{k}_{d2}^{o} - \boldsymbol{K} - \boldsymbol{\eta}^{o}, \\ \boldsymbol{k}_{a2}^{o} &= \boldsymbol{k}_{i2}^{e} + \boldsymbol{K} + \boldsymbol{\eta}^{e}. \end{aligned} \tag{6}$$

The first equation described the formation of the side maximum during diffraction of the o-polarised wave in the

first AO cell (ray 5 in Fig. 2), the second – scattering of light from the first diffraction order in the first cell in the second AO filter (ray 8) and the third – diffraction of e-polarised ray 3 propagated through the first cell with the formation of ray 9. Note that the vector triangles in Fig. 5 described by the first two equations from system (6) exactly coincide. In this case, the wave vectors presented in Fig. 5 correspond to light waves diffracted at the ultrasound wave both in the first and second crystals. The mutual orientation of the AO cells is not taken into account in the vector diagram, while the spatial location of the wave vectors taking into account the configuration of the whole system is chosen according to Fig. 1. After refraction of radiation from the input face of the second crystal, vectors $\boldsymbol{k}'^{\,o}_{a2}$ and $\boldsymbol{k}'^{\,e}_{a1}$ coincide and rays 4 and 7 corresponding to them propagate parallel to each other in air. In the scheme of the ray path in the system of two filters (Fig. 2), the dot-and-dash line shows rays corresponding to the main (wide-aperture) diffraction maxima, while dashed lines show the propagation direction of side rays.

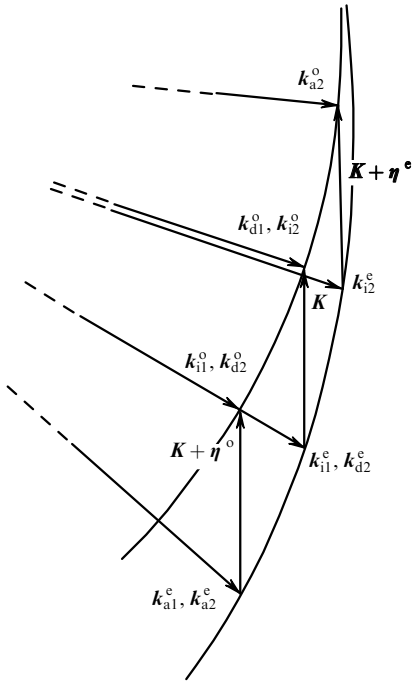

Figure 5. Fragment of the vector diagram with side diffraction maxima.

The diffraction pattern presented in Fig. 2 was observed experimentally. We found that apart from three beams corresponding to the zero and the first diffraction orders, this diffraction pattern also had three beams of a lower intensity. Single side ray 9 propagated to the same side from zero-diffraction ray 6 as rays 4 and 7; on the opposite side from the zero-diffraction ray, two side orthogonally-polarised rays 5 and 8 propagated parallel to each other.

Light diffraction on side components of the angular spectrum of the acoustic field can be treated as diffraction on a plane elastic wave with the wave vector $\boldsymbol{K}$, which is characterised by the nonzero phase mismatch η [1]. It is easy to show that at small divergence angles of the ultrasound wave ($\delta\alpha \ll 1$), this mismatch can be determined by using the expression

$$\eta = \frac{\sin\delta\alpha}{\cos(\psi+\delta\alpha)}\,K \approx \frac{\delta\alpha}{\cos\psi}\,K. \tag{7}$$

Taking into account the fact that the wave number of the ultrasound wave is $K = 2\pi f/V$, the dimensionless mismatch is

$$H = \frac{2f l_{PT}\delta\alpha}{V}. \tag{8}$$

One can see from Fig. 4 that to fulfil the phase-matching condition at one and the same ultrasound frequency $f^* = 65.75$ MHz, it is necessary to rotate the wave vector of the ultrasound wave for the side diffraction maxima in the angular distribution of the ordinary and extraordinary polarised radiation by the angles $\delta\alpha^o = -0.08^\circ$ and $\delta\alpha^e = -0.11^\circ$, respectively. In this case, dimensionless mismatches (8) at the effective length of the acoustic column $l = 0.8$ cm will be as follows: $H^o \approx 3.4$ and $H^e \approx 4.6$. The efficiency of side diffraction determined by expression (4) is approximately the same and rather small for both polarisations of radiation, i.e. $T^o \approx T^e \approx 0.04$.

Transmission function (4) is zero at $H = \pm\sqrt{15} \approx 3.9$ and $\pm\sqrt{35} \approx 5.9$. Therefore, the relation between mismatches H^o and H^e is such that it is impossible to suppress all side diffraction maxima at one and the same length of the piezoelectric transducer. Nonetheless, by choosing the transducer length equal to $l_{PT} \approx 1.5$ cm, it is possible to suppress two side e-polarised rays. In this case, the diffraction efficiency for the third o-polarised ray also decreases and is equal to ~ 0.025.

Thus, the intensity of side diffraction maxima turned to be much smaller than the intensity of the main beams. Side diffraction can be partially suppressed by selecting such a length of the piezoelectric transducer at which the mismatch H for side diffraction would correspond to the local minimum of instrument function (4). It is known also that the special shape of electrodes leads to a decrease in the amplitude of the side lobes of the radiation pattern.

6. Conclusions

In this paper, we have presented the AO system making it possible to perform tunable filtration and modulation of uncollimated arbitrary polarised light beams. The successive use of two identical AO filters has allowed us to realise polarisation-independent AO diffraction of IR radiation and to compensate for birefringence in the zero diffraction order. The high diffraction efficiency at the low driving power, the virtual absence of optical losses and compactness of the control unit make it possible to use the system under study in devices processing optical signals and controlling high-power laser beams.

The research has shown that scattering of light on side components of the angular radiation spectrum in the piezoelectric transducer can lead to the appearance of undesirable orders in the diffraction pattern. In the system under study, the radiation intensity in side maxima does not exceed 4% of the intensity of incident radiation. It is obvious, that the appearance of additional diffraction orders deteriorates the parameters of the system and, as a result, should be taken into account in designing new devices controlling unpolarised light.

References

1. Balakshii V.I., Parygin V.N., Chirkov L.E. *Fizicheskie osnovy akustooptiki* (Physical Foundations of Acousto-optics) (Moscow: Radio i svyaz', 1985).
2. Goutzoulis A., Pape D. *Design and Fabrication of Acousto-Optic Devices* (New York: Marcel Dekker, 1994).
3. Yariv A., Yeh P. *Optical Waves in Crystals* (New York: Wiley, 1984; Moscow: Mir, 1987).
4. Magdich L.N., Molchanov V.Ya. *Akustoopticheskie ustroistva i ikh primenenie* (Acousto-optic Devices and their Applications) (Moscow: Sov. Radio, 1978).
5. Kotov V.M. *Kvantovaya Elektron.*, **21**, 937 (1994) [*Quantum Electron.*, **24**, 874 (1994)].
6. Epikhin V.M., Vizen F.L., Pal'tsev L.L. *Zh. Tekh. Fiz.*, **57**, 1910 (1987) [*J. Tech. Phys.*, **57**, 1910 (1987)].
7. Lee H. *Appl. Opt.*, **27**, 815 (1988).
8. Voloshinov V.B., Molchanov V.Ya. *Opt. Laser Technol.*, **27**, 307 (1995).
9. Voloshinov V.B., Molchanov V.Ya., Babkina T.M. *Zh. Tekh. Fiz.*, **70**, 938 (2000) [*J. Tech. Phys.*, **45**, 1186 (2000)].
10. Voloshinov V.B. *Proc. the First Army Research Laboratory Acousto-Optic Tunable Filter Workshop* (Adelphi, MD, USA: Army Research Laboratory, 1997).
11. Pozhar V.E., Pustovoit V.I. *Kvantovaya Elektron.*, **12**, 2180 (1985) [*Sov. J. Quantum Electron.*, **15**, 1438 (1985)].
12. Pustovoit V.I., Pozhar V.E., Mazur M.M., et al. *Proc. SPIE Int. Soc. Opt. Eng.*, **5953**, 200 (2005).
13. Voloshinov V.B., Magdich L.N., Knyazev G.A. *Kvantovaya Elektron.*, **35**, 1057 (2005) [*Quantum Electron.*, **35**, 1057 (2005)].
14. Antonov S.N. *Zh. Tekh. Fiz.*, **74**, 84 (2004) [*J. Tech. Phys.*, **74**, 84 (2004)].
15. Chang I.C. *Appl. Phys. Lett.*, **25**, 370 (1974).
16. Voloshinov V.B., Mosquera J.C. *Opt. Spekrosk.*, **101**, 675 (2006) [*Opt. Spectrosc.*, **101**, 635 (2006)].